https://doi.org/10.48048/tis.2022.5603

Effect of CuO/rGO and ZnO/rGO Hybrid Additional Layers on Supercapacitor Performance

Santi Rattanaveeranon[1,*] and Knavoot Jiamwattanapong[2]

[1]Applied Physics Material Laboratory, Physics Program, Faculty of Liberal Arts, Rajamangala University of Technology Rattanakosin, Nakhon Pathom 73170, Thailand
[2]Department of General Education-Mathematics, Faculty of Liberal Arts, Rajamangala University of Technology Rattanakosin, Nakhon Pathom 73170, Thailand

([*]Corresponding author's e-mail: santi.r@rmutr.ac.th)

Received: 11 April 2021, Revised: 6 July 2021, Accepted: 13 July 2021

Abstract

Increasing the specific electrical capacitance of supercapacitors has been received great attention from both researchers and industry. Herein, how to achieve this by coating the surface of reduced graphene oxide (rGO) with copper(II) oxide (CuO) and zinc oxide (ZnO) is reported. The CuO/rGO and ZnO/rGO hybrid layers were prepared via chemical reactions between graphene oxide (GO) and salts of copper and zinc, respectively. The crystallographic structures and surface morphologies of composite materials were studied by using X-ray diffraction (XRD) and scanning electron microscopy (SEM), respectively. Cyclic voltammetry (CV) and electrical capacitance measurements were used to analyze the electrochemical properties of the composites. The results show that CuO and ZnO increased the specific electrical capacitance of rGO, while the composite CuO/rGO and ZnO/rGO materials have good chemical stability with a higher specific electrical capacity (465.73 $F \cdot g^{-1}$) than CuO/rGO (167.52 $F \cdot g^{-1}$), ZnO/rGO (185.48 $F \cdot g^{-1}$), rGO (113.50 $F \cdot g^{-1}$), and annealed graphite (53.12 $F \cdot g^{-1}$). The mechanism of increasing the specific capacitance depending on whether the composite CuO/rGO and ZnO/rGO materials act as a pseudocapacitor and/or an electrical double-layer capacitor is elucidated.

Keywords: Reduced graphene oxide, Copper(II) oxide/reduced graphene oxide, Zinc oxide/reduced graphene oxide, Supercapacitor, Cyclic voltammetry

Introduction

An electrochemical capacitor, also known as a supercapacitor, is an energy storage mechanism that is usable and highly secure. It can be used in a variety of ways, such as memory backup in electric cars, backup power for batteries, renewable energy applications, etc. [1]. Several materials used to develop efficient supercapacitors have been studied. Porous carbon, transition metal oxides, and conducting polymers have shown lower potential than composite materials [2]. Transition metal oxides and conducting polymers can improve electrical capacitance based on two mechanisms: Electrical double-layer capacitance (EDLC) and pseudocapacitance. In the former, materials with a high specific surface area store electrostatic charge in the superconductor, while in the latter, the materials create the charge electrochemically [3]. Hybrid electrochemical capacitors have both characteristics. For instance, Zhang *et al*. [4] reported the fabrication of composite materials able to produce higher electrical capacitance and energy than when using just one material.

Graphene comprises carbon atoms with a single-layer sp^2 arrangement that has been studied for many years due to its excellent potential in both fundamental principles and technological applications [2]. Theoretically, the high specific surface area of graphene (2675 $m^2 \cdot g^{-1}$) bestows its EDLC property. Graphene oxide (GO) and reduced GO (rGO), along with other carbon materials such as activated carbon, carbon aerogels, and carbon nanotubes, have been utilized as electrodes in supercapacitors as they show good EDLC, high specific surface area, and chemically stable properties [5].

The processes of charge transfer and EDLC can result in higher capacitance and energy density improvement of EDLC. For example, polymer and metal oxide such as nickel(II) oxide (NiO) [6], ruthenium(IV) oxide (RuO_2) [7], manganese(IV) oxide (MnO_2) [8], cobalt(II, III) oxide (Co_3O_4) [9], and vanadium(V) oxide (V_2O_5) [10]. Copper(II) oxide (CuO) and zinc oxide (ZnO) both have the

pseudocapacitive characteristic, and so combining them with a carbon-based material with the EDLC property produces a hybrid with both types of capacitance and both faradaic and non-faradaic properties. These materials with improved electrochemical properties can be applied to charging and storage applications. ZnO is currently used in several optoelectronic devices, such as photovoltaic cells, gas sensors, and light-emitting diodes due to its combination of electrical and optical properties [11]. CuO is a p-type semiconductor with a narrow bandgap, the antiferromagnetic property, excellent chemical stability, and low cost, and is abundant [12]. It is considered to be an effective electrode material for many applications, including supercapacitors.

In this research, composite materials comprising rGO and either CuO or ZnO were prepared by growing the crystals of CuO and ZnO onto GO plates, followed by applying a reducing chemical reaction to form the CuO/rGO and ZnO/rGO composite materials. They were then coated onto stainless steel electrodes to measure the electrochemical properties of the prototype.

Materials and methods

Synthesis of GO and rGO

GO was prepared by using Hummer's method. In brief, 3 g of graphite powder (20 μm; 99.99 % purity; Lianyungang Jinli Carbon) was heated at 300 °C in an oven for 2 h to remove contaminants. After that, the graphite was rinsed with 69 mL concentrated sulfuric acid (H_2SO_4) and placed in a mixture of 1.5 g of sodium nitrate ($NaNO_3$) and 9 g of potassium permanganate ($KMnO_4$) in an ice bath (below 20 °C), which produced a gray sediment. The mixture was stirred in a 1,000 mL beaker to which 420 mL of deionized water was added and the temperature raised to 50 °C. Following this, the mixture was stirred at room temperature for 30 min, after which 3 mL of 30 % H_2O_2 was slowly added while stirring until the solution turned yellow-brown. This was then set aside for a moment to allow precipitation to occur. The yellow-brown solution was removed with a pipette and then filtrated and washed with deionized water until the pH of the eluate was around 7 to afford GO.

The GO was then used to prepare rGO. The 36 g of GO were mixed with hydrazine monohydrate ($NH_2NH_2{\cdot}H_2O$) at a ratio of 3 mg/mL. (GO: $NH_2NH_2{\cdot}H_2O$) in a 500 mL round bottom flask, and then stirred at 80 °C for 12 h using a reflux method. Finally, the black rGO precipitate was filtered out and washed several times with deionized water until the pH of the eluate was around 7. Finally, the rGO was dried at 80 °C for 6 h.

Synthesis of CuO/rGO

The 36 mg of dried GO powder was dissolved in 30 mL of deionized water, to which 0.2 M $CuCl_2$ was added. Afterward, 30 mL of 0.1 M sodium hydroxide (NaOH) were carefully added dropwise into the mixture at a constant rate of 50 drops/min while stirred quickly until the mixture was homogeneous. Next, 12 mL of $NH_2NH_2{\cdot}H_2O$ was added, followed by ultrasonication for 10 min and then heating at 80 °C for 30 min. The precipitate was filtered with deionized water several times until the pH of the eluate was close to 7. Finally, the CuO/rGO powder obtained was dried at 80 °C for 2 h in ambient air.

Synthesis of ZnO/rGO

GO at a concentration of 2.5 mg/mL was mixed with 30 mL 0.05 M NaOH added dropwise at 20 drops/min using a burette. On the other side of the beaker, 20 mL of 0.5 M $ZnCl_2$ solution was added while stirred quickly at 700 cycles/min at 70 °C for 20 min, which was then allowed to cool. The sediment was then filtered out and leached with deionized water until the pH of the eluate was close to 7.

Spectroscopic measurements

The composite materials GO, rGO, CuO/rGO, and ZnO/rGO were dropped onto glass slide substrates and then dried on a hotplate before characterization. Field emission SEM (FESEM, Hitachi, s-4700) was used to study the surfaces of the materials. XRD (Bruker D8 Advance diffractometry with Cu Kα radiation) with a low scan rate of 0.021 °/s was used to study the structure of the composite materials. Functional groups in the composite materials were identified by using Fourier-transform spectroscopy (FTIR, Thermo) by mixing them with 0.02 g of potassium bromide (KBr) powder and scanning at wavenumbers from 4,000 - 1,000 cm^{-1}.

Electrochemical measurements

These were carried out at 2 $mol{\cdot}L^{-1}$ using a 2-electrode system in which the composite material had a surface area of 1×1 cm^2 with potassium hydroxide (KOH) as the electrolyte. The electrochemical properties

of the material preparation were measured by using cyclic voltammetry (CV) and the galvanostatic charge-discharge (GCD) technique on a Versastat3 galvanostatic workstation. The materials (GO, rGO, CuO/rGO, and ZnO/rGO) were first coated onto the electrode to afford an active material weight of around 0.25 mg.

Results and discussion

Characteristics of CuO and ZnO on rGO

The SEM image of a thin GO film, **Figure 1(a)**, shows that it comprises very thin regions of graphene platelets, appearing as dark portions and also thicker regions that are folded and wrinkled, appearing as bright regions. Higher magnification views of the thin and thick regions are given in **Figure 1(b)**; the thin regions show smooth areas while the thick regions show folded mass and aggregates [13]. **Figure 1(c)** and **(d)** show the CuO and ZnO crystals on the rGO sheets, respectively. The particle distribution sizes of CuO and ZnO averaged from 100 particles by using the Imagej software program were 66.48 ± 11.23 and 85.15 ± 5.25 nm, respectively. The CuO granules were randomly distributed on the surface of the rGO sheets due to rGO having a large density of oxygen-based functional groups.

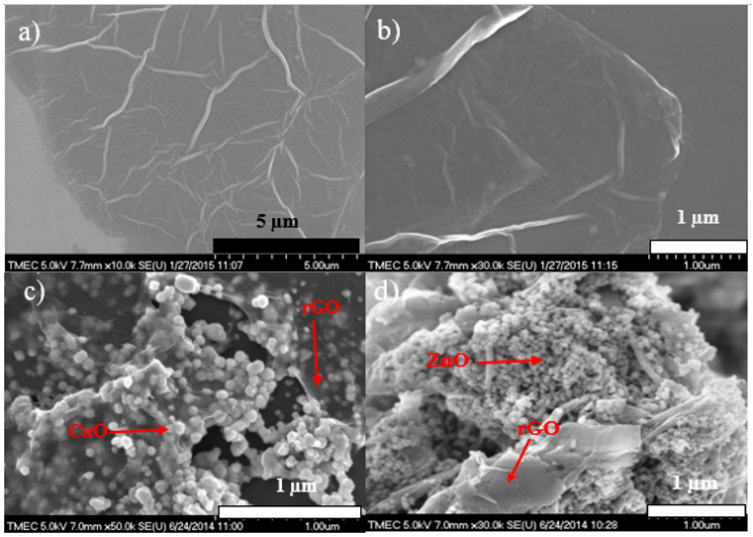

Figure 1 SEM analysis: (a) low-resolution, (b) high-resolution SEM images of GO, SEM image of (c) CuO/rGO and (d) ZnO/rGO.

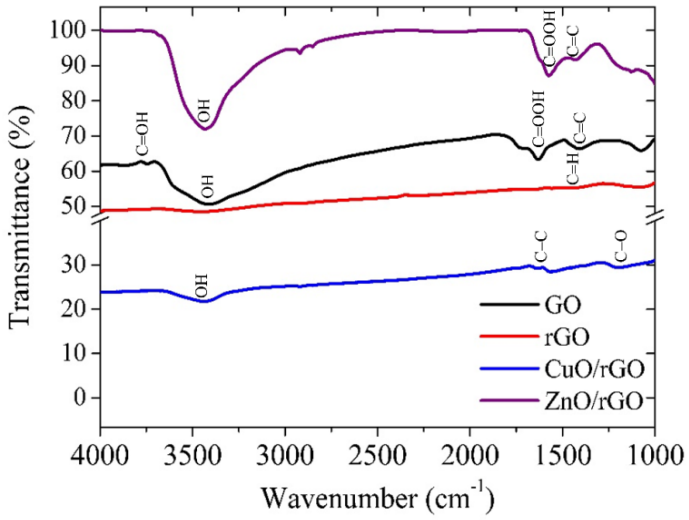

Figure 2 FTIR spectra of GO, rGO, CuO, ZnO, CuO/rGO, and ZnO/rGO.

Figure 2 illustrates that the FTIR analysis identified various functional groups in GO, rGO, CuO, ZnO, CuO/rGO, and ZnO/rGO. C=OH, OH, C=OOH, and C=C bonds produced by the synthesis process were found in the FTIR spectrum for GO, which were not present in that of rGO. Meanwhile, vibrations of C-C and C-O bonds present in the CuO/rGO composite spectrum were produced by Cu^{2+} being oxidized to CuO and then adhering by static electricity to the rGO plates during the chemical preparation. Notice also that OH oscillation appeared at 3,464 cm^{-1}. The FTIR spectrum ZnO/rGO shows that rGO reacting with Zn led to the formation of OH, C=O, C=OOH, and C=C groups [14].

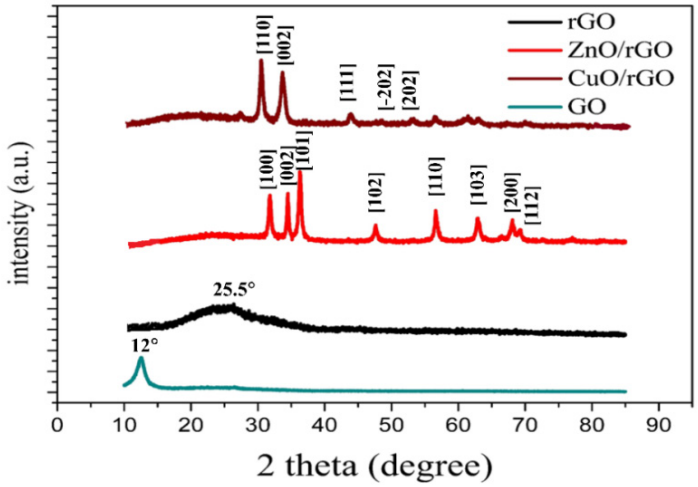

Figure 3 XRD patterns for GO, rGO, CuO, ZnO, CuO/rGO, and ZnO/rGO.

The XRD pattern for GO in **Figure 3** shows a major peak at 20 = 12. This is absent in the XRD pattern for amorphous rGO, which instead, has a wide peak at 20 = 25.5. The diffraction peaks in the XRD pattern for ZnO/rGO corresponded to the hexagonal wurtzite structure of ZnO (ICSD No. 98-002-7781) [10]. When GO reacts with $ZnCl_2$ and NaOH, it forms colloids of zinc hydroxide hexahydrate ($Zn(OH)_2{\cdot}6H_2O$). These can dissolve to produce Zn^{2+} and OH^- during the reduction reaction between OH^- and Zn^{2+} (Eq. (1)) [21]. This caused ZnO nuclei to grow on the surface of the GO sheets.

$$ZnCl_2(aq) + 2NaOH(aq) \rightarrow Zn(OH)_2(aq) + 2NaCl(aq) \quad (1)$$

$$Zn(OH)_2(s) \rightarrow ZnO(s) + H_2O(l) \quad (2)$$

The diffraction peaks in the XRD pattern of the CuO/rGO composite preparation corresponded to the hexagonal structure of CuO, as confirmed via JCPDS No. 05-0661 [16]. When GO reacts with $CuCl_2$ and NaOH, it forms the colloids of copper(II) hydroxide hexahydrate ($Cu(OH)_2{\cdot}6H_2O$). These can dissolve to produce Cu^{2+} and Cl^- during the reduction reaction between OH^- and Cu^{2+} (Eq. (3)) [22]. This caused CuO nuclei to grow on the surfaces of the GO sheets.

$$CuCl_2(aq) + 2NaOH(aq) \rightarrow 2NaCl(aq) + Cu(OH)_2(aq) \quad (3)$$

$$Cu(OH)_2(s) \rightarrow CuO(s) + H_2O(l) \quad (4)$$

Electrochemical applications

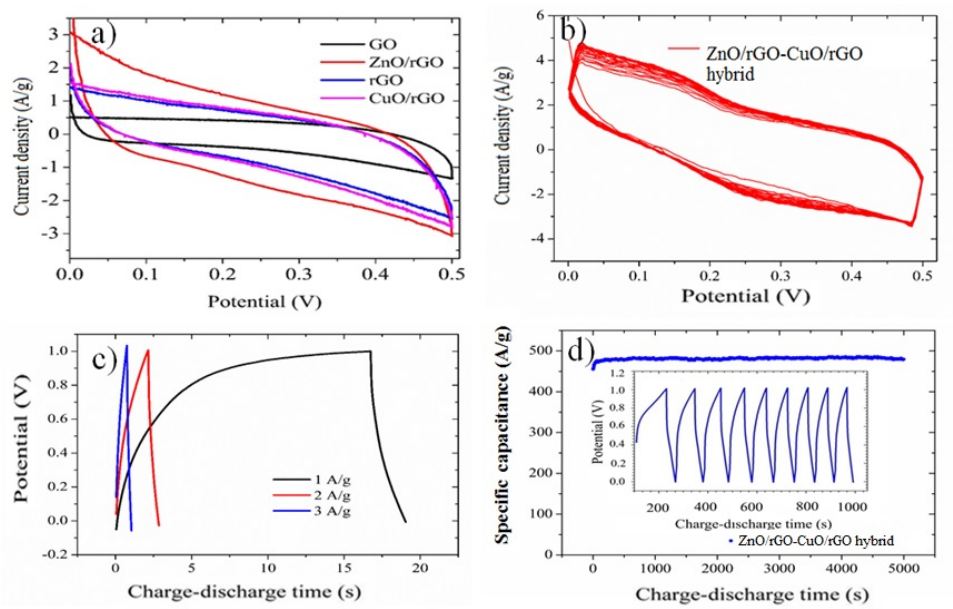

Figure 4 CV curves of (a) GO, rGO, CuO, ZnO, CuO/rGO, and ZnO/rGO at a constant scan rate at 50 mV/s in 2 M KOH electrolyte and (b) the CuO/rGO and ZnO/rGO hybrid materials over 20 cycles at 50 mV/s in 2 M KOH electrolyte. Charge-discharge curves at various current densities for the supercapacitor prototype fabricated with the CuO/rGO and ZnO/rGO hybrid materials according to (a) potential and (d) specific capacitance.

Figure 4(a) shows CV curves for the various materials under optimal conditions. The ZnO/rGO prototype displayed better electrochemical behavior than the CuO/rGO prototype due to the surface of the ZnO/rGO material being higher. This makes it more active over a short time and allows the electrolyte to penetrate the surface faster. Moreover, the ZnO nanoparticles eliminate defects in the inner rGO plate that cause high resistance. All of these factors increase the electrical conductivity of ZnO/rGO. CuO/rGO can promote redox reactions due to the different oxidation states of Cu. For instance, Cu^{+} in the form of CuO increases the specific electrical capacity of the nano-composite material. The pseudocapacitance characteristic of CuO complements the electrical properties of the EDLC of rGO [17]. Moreover, the high specific capacitance of the rGO sheet surface with the interaction between the CuO nanostructures provides ions for the electrolyte solution, which can improve the efficiency of movement and makes it easier for K^{+} from the KOH solution to be inserted in the electrode material [18]. **Figure 4(b)** displays the CV cycling stability testing of the ZnO/rGO and CuO/rGO materials over 20 cycles, which confirms their excellent stability and reversibility [19]. This could be due to the excellent integration of the ZnO and CuO nanoparticles with the rGO sheets. **Figure 4(c)** shows the potential according to the charge-discharge characteristics of the CuO/rGO and ZnO/rGO prototypes under various current density values. The specific capacitance of the prototype can be calculated from a charge-discharge curve as follows [15];

$$C_s = \frac{I \times \Delta t}{\Delta V \times m} (\mathrm{F \cdot g^{-1}}) \tag{5}$$

where I is the discharge current (A), ΔV is the potential window (V), m is the mass of the active material (mg), and Δt is the charge-discharge time.

The specific capacitance is inversely proportional to the magnitude of the current due to the increase in the potential voltage falls when the current density is increased [20]. **Figure 4(d)** shows the specific capacitance according to charge-discharge time over 5,000 charge/discharge cycles at a scan rate of 15 $\mathrm{mVs^{-1}}$; those of CuO/rGO, rGO/ZnO, and rGO/ZnO-CuO/rGO were 167.52, 185.48, and 465.73 $\mathrm{F \cdot g^{-1}}$, respectively.

Conclusions

CuO/rGO and ZnO/rGO hybrid composites can improve the performances of supercapacitors. The specific capacitance of the CuO/rGO-ZnO/rGO prototype was 465.73 $F \cdot g^{-1}$ over 5,000 charge-discharge cycles. Combining these 2 composites with the pseudocapacitance property and rGO with the EDLC property immensely improved the overall capacitance performance. These excellent properties of the CuO/rGO and ZnO/rGO hybrid materials used as electrodes markedly increased the capacitance of the supercapacitor prototype.

Acknowledgements

This research was supported by research funds from Rajamangala University of Technology Rattanakosin (RMUTR). The authors are grateful to the Department of Physics, King Mongkut's University of Technology Thonburi, Thailand for providing the instruments for measuring the electrochemical properties.

References

[1] V Singh, D Joung, L Zhai, S Das, SI Khondaker and S Seal. Graphene based materials: past, present and future. *Progr. Mater. Sci.* 2011; **56**, 1178-271.

[2] H Wang, J Lin and ZX Shen. Polyaniline (PANi) based electrode materials for energy storage and conversion. *J. Sci. Adv. Mater. Dev.* 2016; **1**, 225-55.

[3] M Harilal, B Vidyadharan, II Misnon, GM Anilkumar, Adrian Lowe, J Ismail, MM Yusoff and R Jose. One dimensional assembly of conductive and capacitive metal oxide electrodes for high-performance asymmetric supercapacitors. *ACS Appl. Mater. Interface.* 2017; **9**, 10730-42.

[4] Y Zhang, X Sun, L Pan, H Li, Z Sun, C Sun and BK Tay. Carbon nanotube-ZnO nanocomposite electrodes for supercapacitors. *Solid State Ionics.* 2009; **180**, 1525-8.

[5] E Frackowiak. Carbon materials for supercapacitor application. *Phys. Chem. Chem. Phys.* 2007; **9**, 1774-85.

[6] R Madhu, V Veeramani, SM Chen, P Veerakumar and SB Liu. Functional porous carbon/nickel oxide nanocomposites as binder-free electrodes for supercapacitors. *Chem. Eur. J.* 2015; **21**, 8200-6.

[7] D Majumdar, T Maiyalagan and Z Jiang. A review on recent progress in ruthenium oxide-based composites for supercapacitor applications. *ChemElectroChem.* 2019; **6**, 4343-72.

[8] W Xiao, H Xia, JYH Fuh and L Lu. Growth of single-crystal α-MnO_2 nanotubes prepared by a hydrothermal route and their electrochemical properties. *J. Power Sources.* 2009; **193**, 935-8.

[9] X Xu, Y Yang, M Wang, P Dong, R Baines, J Shen and M Ye. Straightforward synthesis of hierarchical Co_3O_4@$CoWO_4$/rGO core-shell arrays on Ni as hybrid electrodes for asymmetric supercapacitors. *Ceram. Int.* 2016; **42**, 10719-25.

[10] CY Foo, A Sumboja, DJH Tan, J Wang and PS Lee. Flexible and highly scalable V_2O_5-rGO electrodes in an organic electrolyte for supercapacitor devices. *Adv. Energy Mater.* 2014; **4**, 1400236.

[11] X Zhang, H Fan, J Sun and Y Zhao. Structural and electrical properties of p-type ZnO films prepared by Ultrasonic Spray Pyrolysis. *Thin Solid Films.* 2007; **515**, 8789-92.

[12] Z Endut, W Basirun and M Abd Shukor. Pseudocapacitive performance of vertical copper oxide nanoflakes. *Thin Solid Films*. 2013; **528**, 213-6.

[13] K Bramhaiah and NS John. Facile synthesis of reduced graphene oxide films at the air-water interface and in situ loading of noble metal nanoparticles. *Adv. Nat. Sci.: Nanosci. Nanotechnol.* 2012; **3**, 045002.

[14] F Huang, Y Zhong, J Chen, S Li, Y Li, F Wang and S Feng. Nonenzymatic glucose sensor based on three different CuO nanomaterials. *Anal. Methods.* 2013; **5**, 3050-5.

[15] ER Ezeigwe, MTT Tan, PS Khiew and CW Siong. One-step green synthesis of graphene/ZnO nanocomposites for electrochemical capacitors. *Ceram. Int.* 2015; **41**, 715-24.

[16] R Kumar, P Rai and A Sharma. Facile synthesis of Cu_2O microstructures and their morphology dependent electrochemical supercapacitors properties. *RSC Adv.* 2016; **6**, 3815-22.

[17] W Ly, DM Tang, YB He, CH You, ZQ Shi, XC Chen, CM Chen, PX Hou, C Liu and QH Yang. Low-temperature exfoliated graphenes: vacuum-promoted exfoliation and electrochemical energy storage. *ACS nano.* 2009; **3**, 3730-6.

[18] F Wang, S Xiao, Y Hou, C Hu, L Liu and Y Wu. Electrode materials for aqueous asymmetric supercapacitors. *RSC Adv*. 2013; **3**, 13059-84.
[19] S Liu, J Wu, J Zhou, G Fang and S Liang. Mesoporous $NiCo_2O_4$ nanoneedles grown on three dimensional graphene networks as binder-free electrode for high-performance lithium-ion batteries and supercapacitors. *Electrochim. Acta.* 2015; **176**, 1-9.
[20] E Mitchell, A Jimenez, RK Gupta, BK Gupta, K Ramasamy, M Shahabuddin and SR Mishra. Ultrathin porous hierarchically textured $NiCo_2O_4$/graphene oxide flexible nanosheets for high-performance supercapacitors. *New J. Chem.* 2015; **39**, 2181-7.
[21] ME McMahon, RJ Santucci and JR Scully. Advanced chemical stability diagrams to predict the formation of complex zinc compounds in a chloride environment. *RSC Adv*. 2019; **9**, 19905-16.
[22] I Puigdomenech and C Taxén. *Thermodynamic data for copper: Implications for the corrosion of copper under repository conditions (No. SKB-TR--00-13).* Swedish Nuclear Fuel and Waste Management, Stockholm, Sweden, 2000.